

A Study of the Combustion Method to Prepare Fine Ferrite Particles

S. Castro, M. Gayoso,[†] and C. Rodríguez

Department of Inorganic Chemistry, Faculty of Chemistry, University of Santiago de Compostela, E-15706 Santiago de Compostela, Spain

Received December 3, 1996; in revised form June 27, 1997; accepted June 27, 1997

A combustion synthesis method was adapted for the efficient preparation of pure barium ferrite particles (BaFe_2O_4 and $\text{BaFe}_{12}\text{O}_{19}$). It is based on the exothermic reaction of the corresponding metal nitrates with a reducing agent (ODH or TFTA) and yields extremely fine-grained ashes that readily convert into pure BaFe_2O_4 and $\text{BaFe}_{12}\text{O}_{19}$ when treated thermally. The composition and microstructure of the so-obtained materials were studied by XRD and TEM, and the best synthesis conditions were established. © 1997 Academic Press

1. INTRODUCTION

Spinel ferrites combine interesting soft magnetic properties with rather high electrical resistivities (1). Fine-particle spinel ferrites, such as BaFe_2O_4 , are useful for the low-temperature preparation of high-density ferrites and as suspension materials for ferromagnetic liquids (2).

Hexagonal magnetic hard ferrites such as $\text{BaFe}_{12}\text{O}_{19}$ are magnetic materials of great scientific and technological interest due to their relatively strong anisotropy and moderate, but still interesting magnetization. They are applied as permanent magnets, in microwave devices or in perpendicular magnetic recording (3). Fine-particle hexagonal ferrites exhibit magnetic properties different from those observed for sintered materials (4, 5).

A wide range of chemical methods have been used to obtain ultrafine mixed oxide particles: the organometallic precursor method, the pyrosol method, chemical coprecipitation, sol-gel, mechanical milling, hydrothermal method, etc. These chemical methods were recently reviewed by Dufour (6).

The combustion method presents some advantages compared to other methods: reagents are very simple compounds, special equipment is not required (pyrex containers are used), dopants can be easily introduced into the final product, and agglomeration of powders remains limited.

This method uses the energy produced by the exothermic decomposition of a redox mixture of metal nitrates with an

organic compound. In the combustion mixture nitrates and the organic compounds behave similarly to conventional oxidants and fuels. The reaction is carried out by dissolving metal nitrates and fuel in a minimum amount of water in a pyrex dish and heating the mixture in order to evaporate water in excess. The resulting viscous liquid foams, ignites, and undergoes a self-sustained combustion, producing ashes containing the oxide product. During the combustion, exothermic redox reactions associated with nitrate decomposition and fuel oxidation take place. Gases such as N_2 , H_2O , and CO_2 evolve, favoring the formation of fine-particle ashes after only a few minutes. The properties of the final product (particle size, surface area, and porosity) depend on the way combustion is conducted. The departure of gases favors the desegregation of the products (increasing the porosity) and heat dissipation (inhibiting the sintering of the products). The exothermicity of the combustion is controlled by the nature of the fuel and the ratio oxidizer/fuel. Fuels are organic compounds, frequently hydrazine derivatives, with N–N bonds that undergo highly exothermic combustion. When fuels are heated in the presence of nitrates, the mixture of gases generated is always hypergolic: it reacts readily with involvement of heat. The stoichiometric composition of the metal nitrate–fuel mixtures is given by the equivalence ratio ϕ_e , which reflects the relative ratio of intramolecular fuel/oxidizer, considering the total reducing and oxidizing power of both fuel and oxidizer compounds (7). The mixture is considered fuel-rich when $\phi_e < 1$, fuel-lean when $\phi_e > 1$, and stoichiometrically balanced when $\phi_e = 1$. Other factors influencing combustion are the evaporation time, the total mass of the redox mixture, the dish capacity, and the amount of water used to dissolve the reagents.

In the recent literature the combustion method has been used to synthesize a wide range of mixed oxides: ferrites, manganites, cobaltites, chromites, titanates, aluminates, ZrO_2 , $\gamma\text{-Fe}_2\text{O}_3$, superconducting oxides, and CeO_2 , among other compounds (8–11).

This paper reports on the synthesis of barium ferrites using the combustion method with oxaldihydrazide (ODH, $\text{C}_2\text{H}_6\text{N}_4\text{O}_2$) and tetraformaltrisazine (TFTA, $\text{C}_4\text{H}_{12}\text{N}_6 \cdot 2\text{H}_2\text{O}$) as fuels. The microstructure of the products is discussed as a function of the combustion conditions.

[†] Deceased.

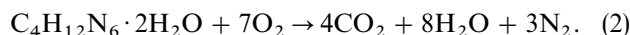
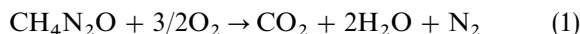
2. EXPERIMENTAL

Two different fuels were used for the combustion: oxal-dihydrazide and tetraformaltrisazine. ODH is a commercial hydrazine derivative, but TFTA must be prepared via the reaction of formaldehyde with hydrazine hydrate as reported earlier (12). We found that the best way to carry out this reaction was the dropwise addition, without stirring, of 240 ml formaldehyde (36.5% aq CH₂O) to a 0°C cooled solution containing 150 ml hydrazide hydrate (80% aq N₂H₄).

Important differences between ODH and TFTA fuels must be pointed out:

(a) Although both of them have N–N bonds, ODH also has C=O bonds that could have some influence on the formation of barium carbonate as a second phase.

(b) Theoretically, complete combustion of 1 mol of ODH gives 7 mol of gases (1), whereas 1 mol of TFTA gives 15 mol of gases (2):



This means that twice the amount of ODH as compared to TFTA is required to produce the same quantity of gases.

In this work mixtures with $\phi_e = 1$ (theoretical value to obtain complete combustion) and $\phi_e < 1$ (fuel-rich mixtures) have been used. Similar amounts of metal nitrates have been used for all samples.

2.1. Combustion Synthesis of Barium Monoferrite BaFe₂O₄

For all samples, barium nitrate Ba(NO₃)₂ (0.405 g) and iron nitrate Fe(NO₃)₃ · 9H₂O (1.250 g) were first dissolved in the minimum amount of water. Either ODH or TFTA was then added to the resulting solution (see Table 1 for amounts). The mixture was heated in an open vessel at a temperature of approximately 300°C.

TABLE 1

Amount of Reducing Agent and Equivalence Ratio (ϕ_e) Used for the Preparation of BaFe₂O₄ and BaFe₁₂O₁₉ Sample Series

Sample	Reducing agent quantity (g)	ϕ_e	
BaFe ₂ O ₄	ODH:	0.730	1
		1.000	0.82
		1.460	0.67
	TFTA:	0.319	1
BaFe ₁₂ O ₁₉	ODH:	3.466	1
		6.932	0.68
		1.544	1
	TFTA:	3.088	0.55

TABLE 2
Proportion (in %) of Impurity Phases Present in BaFe₁₂O₁₉ Samples as Obtained by Rietveld Adjustments of X-Ray Powder Diffraction Patterns

Cumulative thermal treatments	ϕ_e	Reducing agent			
		ODH		TFTA	
		α -Fe ₂ O ₃	BaFe ₂ O ₄	α -Fe ₂ O ₃	BaFe ₂ O ₄
700°C/100 h	= 1	5.4	1.2	25.2	10.4
	< 1	2.5	0.0	13.0	3.8
750°C/100 h	< 1	1.4	0.0	7.8	2.1
850°C/100 h	< 1	0.0	0.0	1.6	0.0

When ODH is used, a viscous green mass is formed after evaporation that decomposes with frothing and foaming before combustion. Then, it ignites, typically after 2 or 3 min. In the case of TFTA combustion is faster and takes place within 30 s only.

Ashes obtained with the first fuel are brown and more porous than those obtained with TFTA.

These ashes were then heat treated as indicated in Table 2.

2.2. Combustion Synthesis of Barium Hexaferrite BaFe₁₂O₁₉

Mixtures of barium nitrate Ba(NO₃)₂ (0.405 g) and iron nitrate Fe(NO₃)₃ · 9H₂O (7.500 g) were dissolved in a minimum amount of water (50 ml), fuel was added to the solution (see Table 1 for quantities), and the final mixtures were heated at a temperature of approximately 300°C.

With ODH a viscous yellow liquid is formed upon evaporation and then, just before combustion, a viscous black product appears whereas a brown viscous mixture is first obtained with TFTA and then a faster and more violent combustion reaction takes place.

In both cases, the ashes obtained after ignition were reddish–brown, but they were more voluminous, more porous, and lighter with ODH than with TFTA, and also when using $\phi_e > 1$, rather than $\phi_e = 1$. These ashes were then heat treated as indicated in Table 2.

2.3. Structural Characterization

X-ray diffraction (XRD) spectra were recorded with a PW-1729 Philips powder diffractometer using CuK α radiation. All patterns were recorded at room temperature, in the step-scan mode. A Rietveld refinement of the X-ray powder diffraction patterns of the well-crystallized samples was carried out using the FULLPROF (13) and ARIT4 (14) programs. The morphological features of the powders were observed with a Philips CM-12 transmission electron microscope, operating at 100 kV.

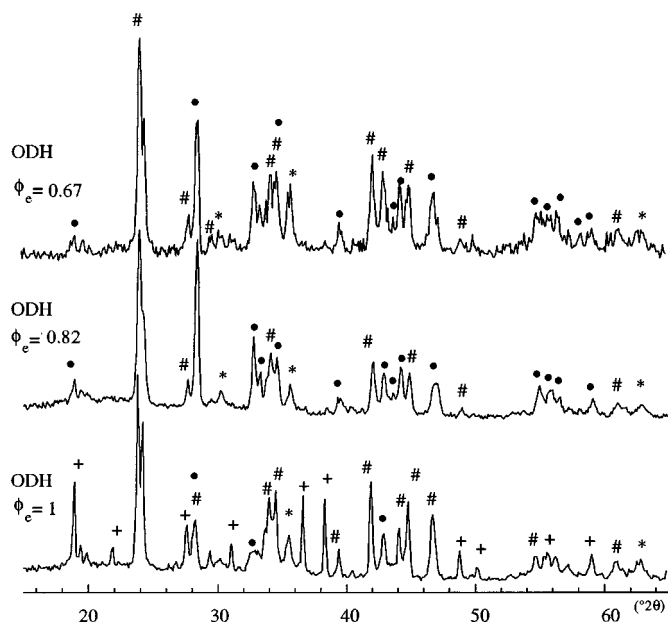


FIG. 1. X-ray powder diffraction patterns of BaFe_2O_4 ash samples. (*) Fe_3O_4 , (+) $\text{Ba}(\text{NO}_3)_2$, (#) BaCO_3 , (●) BaFe_2O_4 .

3. RESULTS AND DISCUSSIONS

The XRD patterns of the ashes obtained after combustion exhibit broad Bragg peaks (Figs. 1 and 2). This broadening was attributed to the small size of the particles and to their poor crystallinity. Electron transmission micrographs of these ashes clearly showed that they are nanoparticles with an average diameter of 70 nm (Fig. 3).

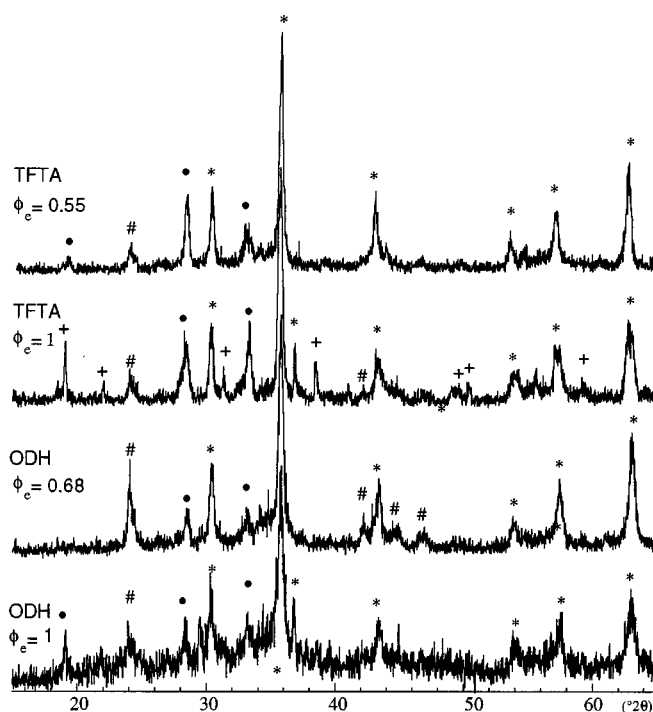


FIG. 2. X-ray powder diffraction patterns of $\text{BaFe}_{12}\text{O}_{19}$ ash samples. (*) Fe_3O_4 , (+) $\text{Ba}(\text{NO}_3)_2$, (#) BaCO_3 , (●) BaFe_2O_4 .

3.1. Barium Monoferrite BaFe_2O_4 Samples

All the ashes obtained after combustion contain Fe_3O_4 , $\text{Ba}(\text{NO}_3)_2$, BaCO_3 , and BaFe_2O_4 in different proportions depending on the sample (Fig. 1). In the samples prepared

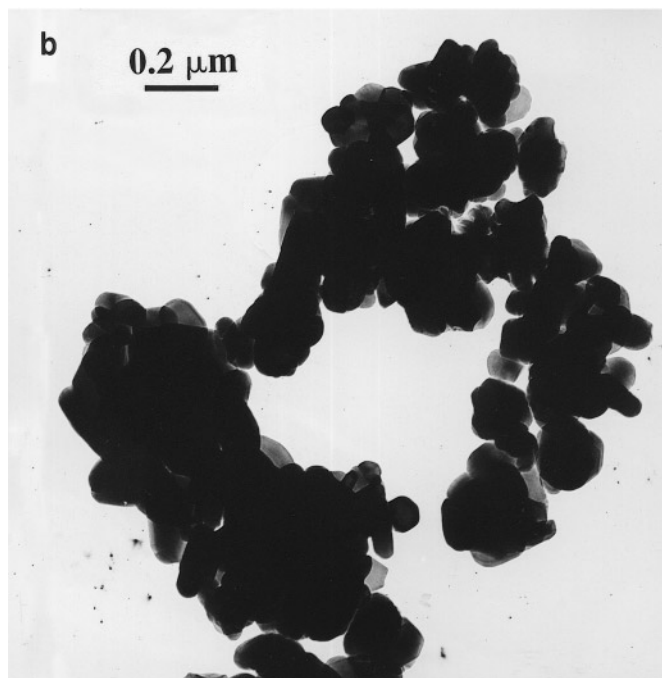
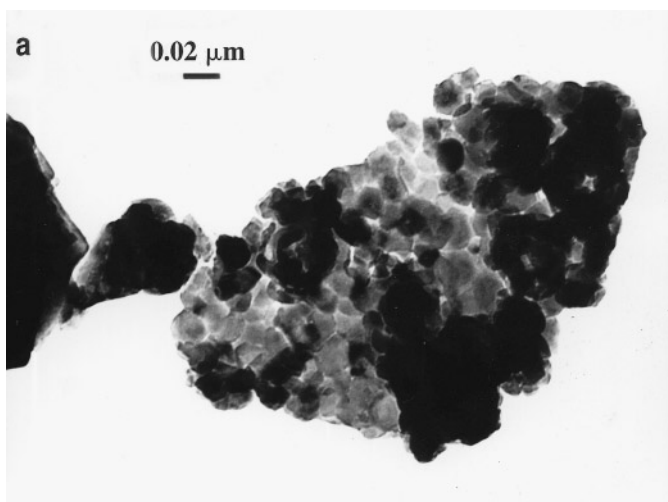


FIG. 3. TEM micrographs of $\text{BaFe}_{12}\text{O}_{19}$: (a) ash samples; (b) samples treated at $700^\circ\text{C}/100$ h.

with ODH:

— BaFe_2O_4 is the main phase when $\phi_e = 0.82$; it is less abundant when $\phi_e = 1$ and $\phi_e = 0.67$.

— $\text{Ba}(\text{NO}_3)_2$ is abundant in the sample prepared with the smallest amount of reducing agent ($\phi_e = 1$).

— BaCO_3 is present in all samples; its relative proportion increases when a larger amount of $\text{Ba}(\text{NO}_3)_2$ has reacted ($\phi_e = 0.67$).

— Fe_3O_4 : no significant differences among the different samples.

The X-ray pattern of the ash sample obtained with TFTA is similar to that of the sample obtained with ODH with $\phi_e = 1$. The conclusion is that fuel-rich mixtures favor the formation of BaFe_2O_4 during the combustion; but if the fuel/oxidizer ratio becomes too high the reaction gets retarded, i.e., it cannot be too fuel-rich. On the other hand experimental results also indicate that smaller water volume and faster evaporation favor the formation of the monoferrite: samples containing the same amount of nitrates and the same fuel/oxidant ratio, but dissolved in a larger amount of water, give a slower combustion reaction and yield less BaFe_2O_4 .

After these ashes have been treated at 700°C for 2 h (Fig. 4), BaFe_2O_4 becomes the major phase in all samples. Nevertheless secondary phases, BaCO_3 and Fe_3O_4 , can still be found. They are more abundant when fuel-lean rather than fuel-rich proportions are used, independently of the nature of the fuel, ODH or TFTA. This result also shows that the presence of C=O bonds in ODH does not promote the formation of more BaCO_3 in the final products.

3.2. Barium Hexaferrite $\text{BaFe}_{12}\text{O}_{19}$ Samples

With this route, as for the commonly used methods, the formation of barium hexaferrite takes place through the

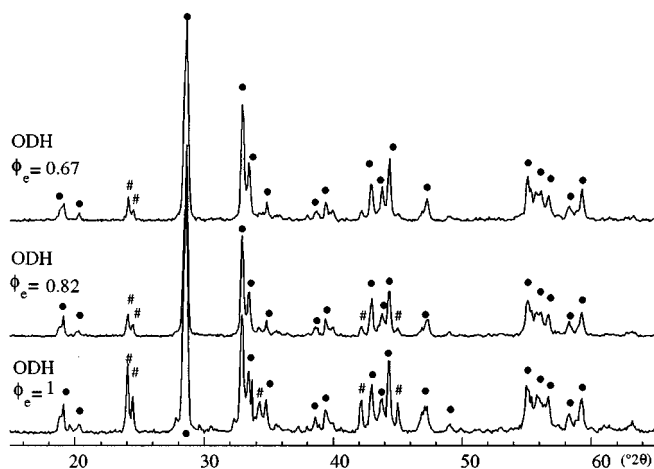
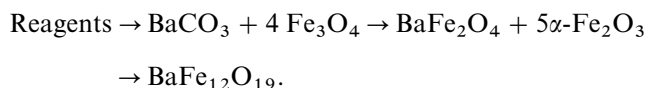


FIG. 4. X-ray powder diffraction patterns of BaFe_2O_4 treated at $700^\circ\text{C}/2$ h. (#) BaCO_3 , (●) BaFe_2O_4 .

following steps:



During the combustion process the precursor phases for the formation of barium hexaferrite were formed. The X-ray patterns of all ashes show the presence of broad peaks that correspond to spinel Fe_3O_4 , BaCO_3 , BaFe_2O_4 (Fig. 2).

More crystalline phases are obtained with ODH for fuel-rich redox mixtures (sample with $\phi_e = 0.68$ more crystalline than sample with $\phi_e = 1$). Thus, a fuel-rich redox reaction improves the combustion reaction.

Combustion with TFTA gives ashes with a slightly better crystallinity containing a larger amount of BaFe_2O_4 .

A large amount of $\text{BaFe}_{12}\text{O}_{19}$ is formed after annealing the ashes at 700°C for 4 h. Well-defined Bragg peaks indicate good crystallinity (Fig. 5). Secondary phases, identified as $\alpha\text{-Fe}_2\text{O}_3$ and BaFe_2O_4 , are also present (Fig. 5). Upon heating of these materials at 700°C for 100 h, the amount of these impurities decreases below 10% for samples prepared with ODH. The impurity level remains high when the sample is prepared with TFTA, about 40% in samples prepared with the smallest amount of fuel and 20% in the other samples (see Table 2). Minor phases were almost eliminated (to less than 1%) upon heating ODH samples to

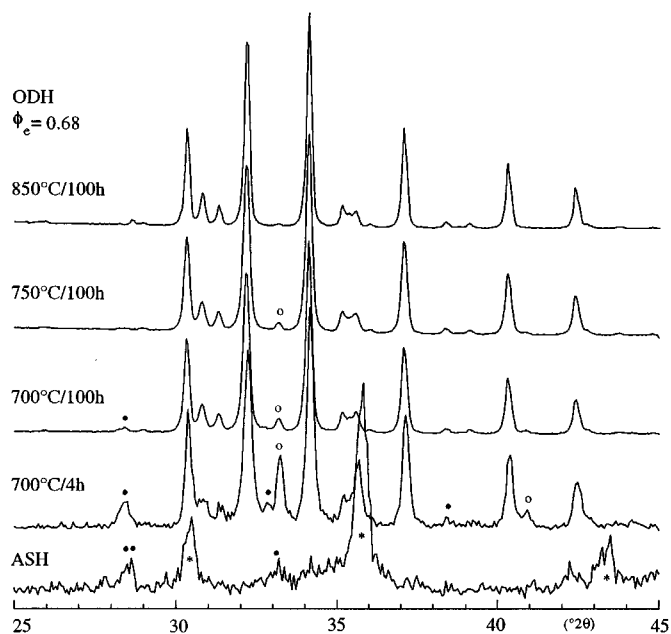


FIG. 5. X-ray powder diffraction patterns of $\text{BaFe}_{12}\text{O}_{19}$ samples obtained with ODH ($\phi_e = 0.68$) treated at different temperatures. (*) Fe_3O_4 , (O) $\alpha\text{-Fe}_2\text{O}_3$, (●) BaFe_2O_4 . The rest of the peaks correspond to the $\text{BaFe}_{12}\text{O}_{19}$ phase.

850°C. TFTA samples always have more impurities than ODH samples after the corresponding treatments (see Table 2).

Electron transmission micrographs clearly show nanostructured particles, with an average diameter of 70 nm, for samples treated at low temperature (Fig. 6). The size of the particles increases slightly with the annealing temperature: for treatments at 750, 850, and 1000°C, average diameters are 0.1, 0.3 and 0.5 μm , respectively. These micrographs do not show any obvious differences in the granulometry of the samples prepared with different fuels and different oxidizer to fuel ratios. As-prepared particles are agglomerated due to sintering. They are more spherical at low temperature and become platelet-like when heated at higher temperature.

3.3. Discussion

We have shown that BaFe_2O_4 and $\text{BaFe}_{12}\text{O}_{19}$ can be obtained via the combustion method. In the successful synthesis of these ferrites it is important to choose the right fuel and oxidizer/fuel ratio. Optimum values of ϕ_e for ODH and TFTA turn out to be less than one in both cases. Larger ϕ_e values can be used to prepare $\text{BaFe}_{12}\text{O}_{19}$ with ODH as a fuel. But with TFTA, samples must be prepared with a ϕ_e very close to the optimum value. So in this case it is easier to use ODH than TFTA. Also ODH is a commercial product while TFTA must be synthesized. And as has been shown, the C=O bond in ODH has no influence on the formation of BaCO_3 phase as an impurity. Thus, ODH is a more convenient fuel than TFTA for the $\text{BaFe}_{12}\text{O}_{19}$.

On the other hand, the volume of ashes prepared using TFTA is lower than that of ashes obtained using ODH. This difference is attributed to the choice of the fuel (15), which alters the exothermicity of the reaction and, consequently, the morphological characteristics of the oxides. The degree of porosity depends directly on the amount of gases that escapes during combustion. A large amount of gases dissipates the heat thereby preventing the oxides from sintering. Also, as the gas escapes, it leaves a porous network for the final product. Consequently ashes obtained from fuel-rich redox mixtures were found to be more porous than those obtained from stoichiometric mixtures ($\phi_e = 1$). For fuel-rich mixtures, no differences are observed in ashes obtained with ODH or TFTA. In the case of stoichiometric mixtures ($\phi_e = 1$), ashes prepared with TFTA are less reactive than those obtained with ODH. This should be due to the fact that the exothermicity of the combustion is not completely compensated by the escaping gases. It also must be pointed out that when evaporation conditions are changed (e.g., temperature, time, volume) the results are also slightly changed: minor temperature, more time or more volume undergo slower evaporation and poor combustion.

4. CONCLUSIONS

Fine particles of barium monoferrite and barium hexaferrite have been prepared by a combustion process. This method offers advantages over other methods for the synthesis of ferrites. Nanosized and very reactive particles of precursor oxides can be prepared rapidly and simply when fuels and the stoichiometry are properly chosen. Consequently, very fine particles can be obtained after a thermal treatment of these precursor oxides. Fuel-rich mixtures favor the formation of barium monoferrite and barium hexaferrite when ODH or TFTA is used as fuel. ODH has some advantages over TFTA: it is a commercial product and it is easier to use an adequate proportion nitrates/fuel.

The magnetic performances of the $\text{BaFe}_{12}\text{O}_{19}$ particles resulting from annealing around 850°C are promising (4 5 16): the main magnetic characteristics (magnetization value of 57.8 emu/g and coercive fields of 5285 Oe at 13.5 kOe) should be due to the high purity (<1% of impurities), the good crystalline state, and the small homogeneous size of the particles (the dimensions of platelet-shaped particles are in the range 0.1–0.2 μm).

ACKNOWLEDGMENTS

We thank M. A. Señaris-Rodríguez for helpful discussions. S. Castro acknowledges the financial support of Galician Government (Spain).

REFERENCES

1. F. Kools and D. Stoppels, "Kirk-Othmer Encyclopedia of Chemical Technology," 4th ed., Vol. 10, Ferrites, Wiley, New York, 1994.
2. P. J. Slick, "Ferromagnetic Materials" (E. P. Wohlfarth, Ed.), Vol. 2, p. 189, North-Holland, Amsterdam, 1980.
3. V. Enz, "Ferromagnetic Materials" (E. P. Wohlfarth, Ed.), Vol. 3, p. 3, North-Holland, Amsterdam, 1982.
4. S. Castro, M. Gayoso, J. Rivas, J. M. Greneche, J. Mira, and C. Rodríguez, *J. Magn. Magn. Mater.* **152**, 61 (1996).
5. S. Castro, M. Gayoso, C. Rodríguez, J. Mira, J. Rivas, S. Paz, and J. M. Greneche, *J. Magn. Magn. Mater.* **140**, 2097 (1995).
6. J. Dufour, C. Negro, R. Latorre, F. López-Mateos, and A. Formoso, *Rev. Metal. Madrid*, **31**(2), 111 (1995).
7. S. R. Jain, K. C. Adiga, and V. R. Pai Verneker, *Combust. Flame* **40**, 71 (1981).
8. K. Suresh, N. R. S. Kumar, and K. C. Patil, *Adv. Mater.* **3**(3), 148 (1991).
9. K. Suresh and K. C. Patil, *J. Solid State Chem.* **99**, 12 (1992).
10. S. Sundar Manoharan and K. C. Patil, *J. Solid State Chem.* **102**, 267 (1993).
11. S. Sundar Manoharan, V. Prasad, S. V. Subramanyan, and K. C. Patil, *Physica C* **190**, 225 (1992).
12. E. W. Schmidt, "Hydrazine and its Derivatives," p. 313, Wiley, New York (1984).
13. J. Rodríguez-Carvajal, "FULLPROF Program," Abstr. Satellite Mtg. on Powder Diffraction, XV Congr. Int. Union of Crystallography, p. 127, Toulouse, 1990.
14. H. M. Rietveld, *Acta Crystallogr.* **22**, 151 (1967).
15. S. Sundar Manoharan and K. C. Patil, *J. Am. Ceram. Soc.* **75**(4), 1012 (1992).
16. S. Castro, Doctoral Thesis, University of Santiago de Compostela, Spain, 1994.